Int. J. Solids Structures, 1971, Vol. 7, pp. 1171 to 1198. Pergamon Press. Printed in Great Britain

BEAMS AND SHELLS WITH MOVING LOADS†

C. R. STEELE‡

Department of Aeronautics and Astronautics, Stanford University, Stanford, California

Abstract—The transient response of the Euler–Bernoulli beam and the Timoshenko beam on elastic foundations due to moving loads is reviewed, using, however, a considerably simpler vector formulation with a Laplace rather than Fourier transformation. The problem of a cylindrical shell with an engulfing axisymmetric pressure wave is shown to be generally quite analogous to the Timoshenko beam problem. However, in contrast to the Timoshenko beam, the bar velocity is a "critical" load speed for which the response can become large. This is due to the coupling between axial and radial motion in the cylinder for the long wave-length modes.

An approach to the problems in which material and geometric properties vary is also discussed. The transformed equation is solved by a method of asymptotic expansions; then the inverse Laplace transformation is evaluated by the asymptotic saddlepoint method. The caustics, which are regions of stress and deformation intensification, may be obtained by geometric construction.

INTRODUCTION

WITH the ever-increasing velocities anticipated for future land, sea, air and space vehicles, one can expect a corresponding increase in the number of situations in which the suitability of a structure depends on its ability to withstand the transient effects of a moving load. And, of the biological problems which are attracting an increasing analytical effort, there are some which might have an interpretation as moving load problems, as in the response of the vessel walls to a pressure wave in the blood, and in the transient response of the cochlea. There are several other problems for which the analytic techniques described in this paper are at least promising, as in current efforts to deduce the properties of bones from external measurements of dynamic response.‖

There will be an increase in the capability of computing equipment that should be able to handle any structural response problem by a direct numerical approach. However, the authors and users of such computer programs seem, at least privately, somewhat conservative about the class of problems for which much faith is placed on the results. Particularly in the transient dynamic response problems one is never quite sure whether the peculiar peaks and high frequency components should be there or are due to numerical error. Therefore, it seems worthwhile for the present objective to be a discussion of a restricted class of moving load problems for which analytical results can be obtained by asymptotic methods.

Many investigators have considered moving load problems for which a simple "steady-state" solution can be obtained. However, such a solution often raises more questions than it resolves. Thus we consider, in this paper, a beam or shell initially at rest and then subjected to the moving load. To simplify the analysis the simply-supported, semi-infinite beam or shell is treated. The actual support conditions turn out to be of secondary importance for

† Portions of this work were supported by the Lockheed, Palo Alto, General Research Program and by NASA Grant NGR-05-020-223 to Stanford University.

‡ Associate Professor.

‖ Work in progress by Anliker *et al.* at Stanford University.

the beam on an elastic foundation and for the axisymmetric shell problem; and the finite beam or shell can be treated by adding appropriate "image" solutions.

Dörr [1] was the first to deduce the correct behavior of the head and tail waves generated by a moving load on a semi-infinite Euler–Bernoulli beam. The finite beam was treated in [2] with the aid of the modified saddlepoint method of van der Waerden [3]. This provides a simple description of the transitional behavior at the front of the head wave and at the rear of the tail wave in terms of the Fresnel integrals, and also gives the behavior at the "critical" load velocity. The critical is equal to the minimum phase velocity of the wave trains that can propagate in the beam on a foundation. For subcritical load velocities the transient deformation is localized to regions near a discontinuity in the load distribution, while at supercritical velocities waves are generated which spread out at their group velocities. The wave train with minimum phase velocity has, however, equal phase and group velocities, so, it seems, that the work done on the beam by the load remains localized, giving a response which increases with the square root of time. If we include either damping or the effects of material or geometric nonlinearities as in [4], a steady-state solution is found at the critical load speed. This bound on the response is large in comparison with the static response when there is little damping in a long slender beam, so this load velocity deserves the designation "critical".

Going to the more elaborate Timoshenko beam model, Crandall [5] found that the "steady-state" solution indicated that for a moving concentrated load the shear wave and bar velocities were also "critical", in addition to the lower critical velocity indicated by the E–B beam solution. However, in [6] it was found that, although a steady-state solution does not exist, the shear and bar velocities are not really critical for the transient response of a finite beam to a distributed load.

It was anticipated that the cylindrical shell exposed to an axial engulfing pressure wave would behave as the beam on a foundation. But in the recently completed work [7] a significant difference was found. Due to the coupling between the axial and radial motion in the cylinder, the phase velocity curve for the first mode has a maximum equal to the bar velocity, which occurs at the limit of zero wave-number. The consequence is that the radial load moving at the bar velocity does produce a response which increases with time. Therefore, the critical load velocities are the bar velocity and the lower velocity analogous to the E–B beam critical. The steady state solution for a concentrated load [8] indicates the shear velocity also to be critical; however, the transient solution for a distributed load shows this not to be the case. The moral seems to be that load speeds should not be labeled "critical" or "not critical" prematurely.

In this paper, transient solutions are obtained using a Laplace transformation of the time variable, which turns out to be simpler than the Fourier transform of the space variable used in [2, 6, 7]. The major objective now is the much larger class of problems for which variations in the material and geometry are present. The Laplace transformation of the time variable may still be used. It is shown in [9] that an asymptotic solution of the transformed equation does yield excellent results for the nonhomogeneous wave equation (in one space dimension). Here we show that an asymptotic solution of the transformed equation, with appropriate saddlepoint evaluation of the inversion integral, gives good results for the more difficult problem of a beam with a variable foundation. The general shell of revolution can obviously be treated in a similar manner.

For methods of direct numerical integration of the shell equations, a vector equation involving only one derivative with respect to the space variable is advantageous [10]. It is

becoming more evident that this formulation is also advantageous in analytical treatment. In the present work, the vector formulation provides a substantial notational convenience in handling the problems that are basically analogous but of varying degrees of complexity.

The list of references is by no means complete; however, some related recent papers in the Russian literature are included [18–22].

EQUATIONS FOR BEAMS AND SHELLS

Since the problems of a beam on an elastic foundation and a shell of revolution have many common features, the notation for the familiar stress and deformation quantities is chosen to be the same for both, as shown in Figs. 1(a), (b). For the transverse bending of the Timoshenko beam on an elastic foundation, the equations are

$$-\frac{\partial}{\partial s}\begin{bmatrix} M \\ H \\ \chi \\ h \end{bmatrix} + \begin{bmatrix} 0 & 1 & 0 & 0 \\ 0 & 0 & 0 & k \\ \dfrac{1}{EI} & 0 & 0 & 0 \\ 0 & \dfrac{\mu}{EA} & -1 & 0 \end{bmatrix} \cdot \begin{bmatrix} M \\ H \\ \chi \\ h \end{bmatrix} + \frac{\partial^2}{\partial t^2}\begin{bmatrix} \rho I_\chi \\ \rho A h \\ 0 \\ 0 \end{bmatrix} = \begin{bmatrix} 0 \\ P_H \\ 0 \\ 0 \end{bmatrix} \tag{1}$$

where k is the foundation modulus, E is Young's modulus, E/μ is the equivalent transverse shear modulus, A and I are the area and moment of inertia of the beam cross section, ρ is the density, t is time and s is the length along the beam.

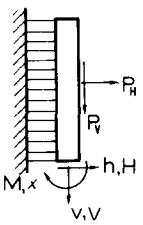

FIG. 1(a). Beam on foundation.

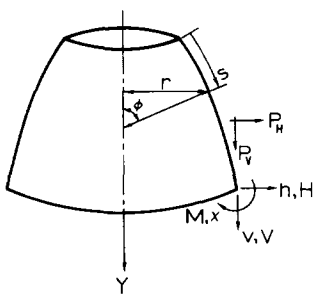

FIG. 1(b). Shell of revolution.

The dimensionless parameter of the problem is

$$\lambda = \left(\frac{EA^2}{kI}\right)_e^{\frac{1}{4}}$$

and the dimensionless length and time are chosen to be

$$x = \frac{s}{\lambda^2}\left(\frac{A_e}{I_e}\right)^{\frac{1}{2}}$$

$$\tau = \frac{t}{\lambda^3}\left(\frac{E_e A_e}{\rho_e I_e}\right)^{\frac{1}{2}}$$

where the subscript e indicates the value at the end of the beam $s = 0$. Equation (1) can be written as

$$-\frac{1}{\lambda}\frac{\partial}{\partial x}\mathbf{v} + \mathbf{A}.\mathbf{v} + \frac{1}{\lambda^2}\mathbf{B}.\frac{\partial^2}{\partial \tau^2}\mathbf{v} = \begin{bmatrix} 0 \\ \dfrac{P_H}{\lambda^2 k_e}\left(\dfrac{A_e}{I_e}\right)^{\frac{1}{2}} \\ 0 \\ 0 \end{bmatrix} \tag{2}$$

where

$$\mathbf{v} = \begin{bmatrix} \dfrac{M}{E_e I_e}\left(\dfrac{I_e}{A_e}\right)^{\frac{1}{2}} \\ \dfrac{H\lambda}{E_e A_e} \\ \dfrac{\chi}{\lambda} \\ \dfrac{h}{\lambda^2}\left(\dfrac{A_e}{I_e}\right)^{\frac{1}{2}} \end{bmatrix}$$

$$\mathbf{A} = \begin{bmatrix} 0 & 1 & 0 & 0 \\ 0 & 0 & 0 & k^* \\ [(EI)^{-1}]^* & 0 & 0 & 0 \\ 0 & \dfrac{\mu}{\lambda^2 (EA)^*} & -1 & 0 \end{bmatrix}$$

$$\mathbf{B} = \begin{bmatrix} 0 & 0 & \dfrac{(\rho I)^*}{\lambda^2} & 0 \\ 0 & 0 & 0 & (\rho A)^* \\ 0 & 0 & 0 & 0 \\ 0 & 0 & 0 & 0 \end{bmatrix}.$$

For notational convenience, the star indicates that the quantity is normalized with respect to its value at the end of the beam (or shell) $s = 0$

$$f^* = f/f_e.$$

Thus for the homogeneous problem any starred quantity is unity.

When the beam is stiff in comparison with the foundation, which is the situation for which these equations are generally valid, the parameter λ is large in comparison with unity. If the terms $0(\lambda^{-2})$ are deleted from the matrices **A** and **B** the equations for the Euler–Bernoulli beam model are obtained.

Now we consider a unit step load which moves along a semi-infinite beam which is initially at rest. To admit the possibility of a variable velocity of the load, the time of arrival at the point of the beam x of the load discontinuity is given by the (monotonically increasing) function $\tau = \xi(x)$, which has the inverse $x = \xi^{-1}(\tau)$. Thus the load is

$$\frac{P_H}{\lambda^2 k_e}\left(\frac{A_e}{I_e}\right)^{\frac{1}{4}} = \begin{cases} 1 & \text{for} \quad 0 < \xi(x) < \tau \\ 0 & \text{for} \quad \tau < \xi(x). \end{cases}$$

The Laplace transformation

$$\bar{\mathbf{v}}(x, p) = \int_0^\infty \mathbf{v}(x, \tau)\, \mathrm{e}^{-p\lambda\tau}\, \mathrm{d}\tau$$

which has the inversion

$$\mathbf{v}(x, \tau) = \frac{\lambda}{2\pi i}\int_{\gamma - i\infty}^{\gamma + i\infty} \bar{\mathbf{v}}(x, p)\, \mathrm{e}^{\lambda p\tau}\, \mathrm{d}p$$

reduces the equation (2) to

$$-\frac{1}{\lambda}\frac{\partial}{\partial x}\bar{\mathbf{v}} + (\mathbf{A} + p^2\mathbf{B})\bar{\mathbf{v}} = \frac{\mathrm{e}^{-\lambda p\xi(x)}}{\lambda p}\mathbf{b} \tag{3}$$

where

$$\mathbf{b} = \begin{bmatrix} 0 \\ 1 \\ 0 \\ 0 \end{bmatrix}.$$

The remaining steps—finding the solution of (3) which satisfies appropriate boundary conditions and then evaluating the integral—are nontrivial, especially for the case of variable properties, so the discussion is postponed to the following sections.

The axial motion of the beam is described by the simple wave equation, completely uncoupled from the transverse bending. For the axisymmetric deformation of the shell of revolution indicated in Fig. 1(b), the axial and radial motions are coupled, as described by the equation

$$\begin{bmatrix} 0 \\ P_H \\ P_v \\ 0 \\ 0 \\ 0 \end{bmatrix} = -\frac{\partial}{\partial s}\begin{bmatrix} M \\ H \\ V \\ \chi \\ h \\ v \end{bmatrix} + \frac{\partial^2}{\partial t^2}\begin{bmatrix} \frac{\delta^3}{12}\rho\chi \\ \delta\rho h \\ \delta\rho v \\ 0 \\ 0 \\ 0 \end{bmatrix} +$$

$$+\begin{bmatrix} -(1-\nu)\dfrac{\cos\varphi}{r} & \sin\varphi & -\cos\varphi & \dfrac{E\delta^3}{12}\dfrac{\cos^2\varphi}{r^2} & 0 & 0 \\ 0 & -(1-\nu)\dfrac{\cos\varphi}{r} & \nu\dfrac{\sin\varphi}{r} & 0 & \dfrac{E\delta}{r^2} & 0 \\ 0 & 0 & -\dfrac{\cos\varphi}{r} & 0 & 0 & 0 \\ \dfrac{12(1-\nu^2)}{E\delta^3} & 0 & 0 & -\nu\dfrac{\cos\varphi}{r} & 0 & 0 \\ 0 & \dfrac{(1-\nu^2)\cos^2\varphi+\mu\sin^2\varphi}{E\delta} & \dfrac{\cos\varphi\sin\varphi(1-\nu^2-\mu)}{E\delta} & -\sin\varphi & -\nu\dfrac{\cos\varphi}{r} & 0 \\ 0 & \dfrac{\cos\varphi\sin\varphi(1-\nu^2-\mu)}{E\delta} & \dfrac{(1-\nu^2)\sin^2\varphi+\mu\cos^2\varphi}{E\delta} & \cos\varphi & -\nu\dfrac{\sin\varphi}{r} & 0 \end{bmatrix} \begin{bmatrix} M \\ H \\ V \\ \chi \\ h \\ v \end{bmatrix} \tag{4}$$

in which δ is the thickness, ν is Poisson's ratio and E/μ is the equivalent transverse shear modulus. In the derivation of these equations, only the first approximation constitutive relations are used. A full discussion is in [11].

An appropriate dimensionless parameter is the usual

$$\lambda = \left[12(1-\nu^2)\frac{r_e}{\delta_e \sin\varphi_e} \right]^{\frac{1}{4}}$$

with the dimensionless arc length and time chosen to be

$$x = \frac{s \sin\varphi_e}{r_e} \qquad \tau = \frac{t}{r_e \lambda}\left(\frac{E_e}{\rho_e}\right)^{\frac{1}{2}}.$$

Then (4) becomes

$$-\frac{\partial}{\lambda \partial x}\mathbf{v} + \mathbf{A}.\mathbf{v} + \frac{1}{\lambda^2}\mathbf{B}.\frac{\partial^2}{\partial \tau^2}\mathbf{v} = \mathbf{a} \tag{5}$$

where the vector of stress and deformation quantities is

$$\mathbf{v} = \begin{bmatrix} \dfrac{M}{E_e \delta_e^2}[12(1-\nu^2)]^{1/2} \\ \dfrac{H\lambda \sin\varphi_e}{E_e \delta_e} \\ \dfrac{V\lambda \sin\varphi_e}{E_e \delta_e} \\ \chi\lambda^{-1} \\ \dfrac{h}{r_e} \\ \dfrac{v}{r_e} \end{bmatrix}$$

and the matrix $\mathbf{A}$ is

$$\mathbf{A} = \mathbf{A}_0 + \frac{1}{\lambda}\mathbf{A}_1 + \frac{1}{\lambda^2}\mathbf{A}_2$$

$$= \begin{bmatrix} 0 & (\sin\varphi)^* & -\dfrac{\cos\varphi}{\sin\varphi_e} & 0 & 0 & 0 \\ 0 & 0 & 0 & 0 & (E\delta/r^2)^* & 0 \\ 0 & 0 & 0 & 0 & 0 & 0 \\ [(E\delta^3)^{-1}]^* & 0 & 0 & 0 & 0 & 0 \\ 0 & 0 & 0 & -(\sin\varphi)^* & 0 & 0 \\ 0 & 0 & 0 & \dfrac{\cos\varphi}{\sin\varphi_e} & 0 & 0 \end{bmatrix}$$

$$-\frac{1}{\lambda}\frac{r_e\cos\varphi}{r\sin\varphi_e}\begin{bmatrix}1-\nu & 0 & 0 & 0 & 0 & 0\\ 0 & 1-\nu & -\nu\tan\varphi & 0 & 0 & 0\\ 0 & 0 & 1 & 0 & 0 & 0\\ 0 & 0 & 0 & \nu & 0 & 0\\ 0 & 0 & 0 & 0 & \nu & 0\\ 0 & 0 & 0 & 0 & \nu\tan\varphi & 0\end{bmatrix}+\frac{1}{\lambda^2\sin^2\varphi_e}$$

$$\times\begin{bmatrix}0 & 0 & 0 & \cos^2\varphi(1-\nu^2)\left(\dfrac{E\delta^3}{r^2}\right)^* & 0 & 0\\ 0 & 0 & 0 & 0 & 0 & 0\\ 0 & 0 & 0 & 0 & 0 & 0\\ 0 & 0 & 0 & 0 & 0 & 0\\ 0 & \dfrac{(1-\nu^2)\cos^2\varphi+\mu\sin^2\varphi}{(E\delta)^*} & \dfrac{(1-\nu^2-\mu)\cos\varphi\sin\varphi}{(E\delta)^*} & 0 & 0 & 0\\ 0 & \dfrac{(1-\nu^2-\mu)\cos\varphi\sin\varphi}{(E\delta)^*} & \dfrac{(1-\nu^2)\sin^2\varphi+\mu\cos^2\varphi}{(E\delta)^*} & 0 & 0 & 0\end{bmatrix}.$$

The remaining terms of (5) are

$$\mathbf{B}=\begin{bmatrix}0 & 0 & 0 & \dfrac{(1-\nu^2)(\delta^3\rho)^*}{\lambda^2\sin^2\varphi_e} & 0 & 0\\ 0 & 0 & 0 & 0 & (\delta\rho)^* & 0\\ 0 & 0 & 0 & 0 & 0 & (\delta\rho)^*\\ 0 & 0 & 0 & 0 & 0 & 0\\ 0 & 0 & 0 & 0 & 0 & 0\\ 0 & 0 & 0 & 0 & 0 & 0\end{bmatrix}$$

$$\mathbf{a}=\begin{bmatrix}0\\ \dfrac{r_eP_H}{E_e\delta_e}\\ \dfrac{r_eP_v}{E_e\delta_e}\\ 0\\ 0\\ 0\end{bmatrix}.$$

HOMOGENEOUS PROBLEMS

In this section we consider the three successively more difficult problems of the Euler–Bernoulli beam on a foundation, the Timoshenko beam and the cylindrical shell, but in the special case that the geometric and material properties and the load velocity are all constant. In this case, the solution of (3) is relatively simple, since the coefficients are constant. Then once the somewhat tedious problems on the algebra of complex functions are resolved, saddlepoint methods used on the inversion integral yield results which give a clear qualitative picture of the solution and also are useful for explicit calculation in the range of the space and time variable for which any direct numerical approach is excessively expensive.

Euler–Bernoulli beam

When the terms $0(\lambda^{-2})$ are deleted from **A** and **B**, the solution of (3) is easily obtained. The particular solution is

$$\bar{\mathbf{v}} = \frac{e^{-\lambda p\xi}}{\lambda p[(p\xi')^4 + p^2 + 1]} \begin{bmatrix} -(p\xi')^2 \\ (p\xi')^3 \\ p\xi' \\ 1 \end{bmatrix} = \frac{e^{-\lambda p\xi}}{\lambda p[(p\xi')^4 + p^2 + 1]} \boldsymbol{\alpha}(p\xi')$$

where the primes denote differentiation with respect to x. Since $\xi(x)$ gives the arrival time of the load at the point x, ξ' is the reciprocal of the (dimensionless) velocity which is constant in the present consideration. The complementary solutions are

$$\bar{\mathbf{v}} = f(p)\, e^{-\lambda\zeta(x)} \begin{bmatrix} -(\zeta')^2 \\ (\zeta')^3 \\ \zeta' \\ 1 \end{bmatrix} = f(p)\, e^{-\lambda\zeta} \boldsymbol{\alpha}(\zeta')$$

where f is an arbitrary function of p and ζ' is a root of

$$(\zeta')^4 + p^2 + 1 = 0.$$

We will choose ζ' to be the root which has the branch cuts chosen to give the mapping $\zeta' = \zeta'(p)$ shown in Fig. 2. The second root, which has a positive real part for positive p, is $\zeta'_2 = i\zeta'$. The remaining roots are the negatives of ζ' and ζ'_2, but these give solutions which for positive p are unbounded at $x = +\infty$ and therefore must be absent. Thus for the semi-infinite, simply-supported beam the solution of (3) is

$$\bar{\mathbf{v}}(x, p) = \frac{e^{-\lambda p\xi} \boldsymbol{\alpha}(p\xi')}{\lambda p[(p\xi')^2 - (\zeta')^2][(p\xi')^2 - (\zeta'_2)^2]} - \frac{e^{-\lambda\zeta} \boldsymbol{\alpha}(\zeta')}{\lambda p[(p\xi')^2 - (\zeta')^2] 2(\zeta')^2} - \frac{e^{-\lambda\zeta_2} \boldsymbol{\alpha}(\zeta'_2)}{\lambda p[(p\xi')^2 - (\zeta'_2)^2] 2(\zeta'_2)^2}. \tag{6}$$

When (6) is substituted into the inversion integral, we see immediately that the particular solution term gives zero contribution for points ahead of the load $\xi(x) > \tau$, and for $\xi(x) < \tau$,

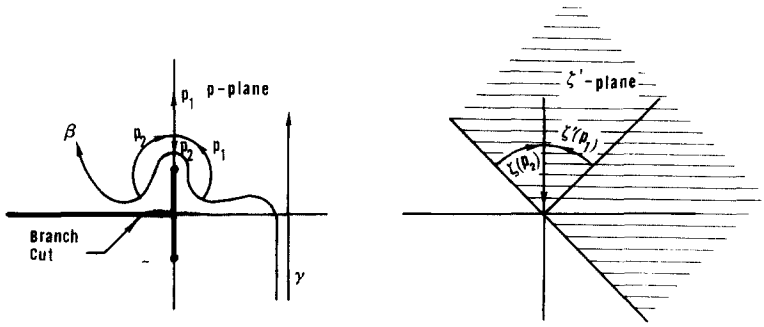

FIG. 2. Mapping of $\zeta' = \zeta'(p)$ showing integration contours γ and β and loci of p_1 and p_2, the zeros of $p\xi' - \zeta'$.

since the contour γ can be deformed to infinity in the negative p direction, gives the residues at the poles $p = 0, \zeta'/\xi'$ and ζ_2'/ξ'.

The two poles, which are the zeros of $p - \zeta'/\xi'$, are denoted by p_1 and p_2

$$p_{1,2} = \left[\frac{-1 \pm [1 - 4(\xi')^4]^{\frac{1}{2}}}{2(\xi')^4}\right]^{\frac{1}{2}}$$

the loci of which are indicated in Fig. 2. For low velocity $\xi' \gg 1$, they are at

$$p_{1,2} \sim \frac{1 \pm i}{2^{\frac{1}{2}}} \frac{1}{\xi'},$$

coalesce at $p_{1,2} = i2^{\frac{1}{2}}$ for $\xi' = 2^{-\frac{1}{4}}$, and remain imaginary for higher velocities

$$p_1 \sim \frac{i}{(\xi')^2} \qquad p_2 \sim i \qquad \text{for} \quad \xi' \ll 1.$$

These two poles of the particular solution are exactly the same as the poles of the complementary solution involving ζ, and therefore can be accounted for by shifting the integration contour of the integral involving ζ from γ to the contour β which is on the left of the two poles, as indicated in Fig. 2. A similar shift in the integration contour occurs for the integral involving ζ_2, for which the poles are in the lower half of the p-plane.

A further simplification comes from the fact that $\zeta_2(p) = \bar{\zeta}(p)$. Thus the integral involving ζ_2 is the negative of the complex conjugate of the integral involving ζ. So the final result for the solution is, for $\xi(x) > \tau$

$$\mathbf{v}(x, \tau) = -\frac{1}{2\pi} \operatorname{Im} \int_\gamma \frac{e^{\lambda(p\tau - \zeta)} \boldsymbol{\alpha}(\zeta')\, dp}{p(\zeta')^2[(p\xi')^2 - (\zeta')^2]} \tag{7a}$$

while for points behind the load front $\xi(x) < \tau$

$$\mathbf{v}(x, \tau) = \begin{bmatrix} 0 \\ 0 \\ 0 \\ 1 \end{bmatrix} - \frac{1}{2\pi} \operatorname{Im} \int_\beta \frac{e^{\lambda(p\tau - \zeta)} \boldsymbol{\alpha}(\zeta')\, dp}{p(\zeta')^2[(p\xi')^2 - (\zeta')^2]}. \tag{7b}$$

The vector giving the uniform displacement under the load comes from the residue of the particular solution at $p = 0$. For a check on the proceedings, we note that at the boundary $x = 0$ there is no branch cut in the first and fourth elements of the integrand of (7b), so the contour β may be deformed to infinity in the negative p direction, leaving only the residue at $p = 0$. The contribution of this residue to the first element of $\mathbf{v}$, the bending moment, is zero, while the contribution to the fourth element, the displacement, cancels the uniform displacement term in (7b). Thus the simple support conditions are satisfied.

Since an exponent with the large parameter λ appears in the integrand of (7), the saddlepoint method may be used to evaluate the integral. The saddlepoint p_s is the zero of the derivative of the argument of the exponent

$$\frac{\tau}{x} = \left(\frac{\partial \zeta'}{\partial p}\right)_{p=p_s}$$

and is a unique point on the positive imaginary axis of the p-plane (for positive values of x/τ). This gives, of course, the group velocity of a wave train with the frequency p_s, and is shown in Fig. 3. The saddlepoint variable $u = u(p)$ is introduced

$$iu^2 = p\tau - \zeta - (p_s\tau - \zeta_s)$$

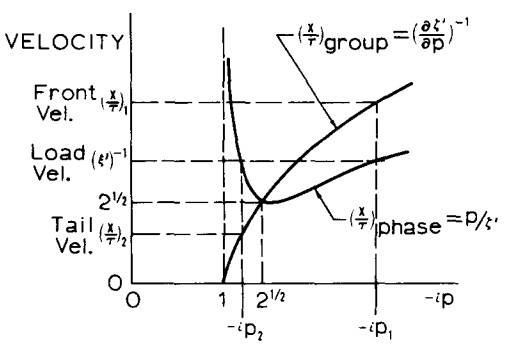

FIG. 3. Phase and group velocities for E–B beam.

so that

$$u(p) = [-i(p\tau - \zeta - p_s\tau + \zeta_s)]^{\frac{1}{2}}$$
$$= \frac{1}{2}\left|\frac{\partial^2 \zeta}{\partial p^2}\right|_s^{\frac{1}{2}} [-i(p - p_s)] + 0[(p - p_s)^2].$$

Thus $u(p)$ is analytic near the saddlepoint, and is positive for values of p on the imaginary axis above the saddlepoint.

The contours γ and β can be deformed to the steepest descent path on which $iu^2 = -|u|^2$ so the most significant contribution comes from the vicinity of the saddlepoint and will be $0(\lambda^{-\frac{1}{2}})$. However, when the pole p_1 is above p_s, the contour γ passes the pole when being deformed to the steepest descent path so the residue must be added, which is $0(1)$. Similarly when the pole p_2 is below p_s, the contour β passes the pole when being deformed to the

steepest descent path, and the residue must be added. All this is more clearly seen from Fig. 3. For a given load velocity, the solution depends primarily on two wave trains with frequencies p_1 and p_2 whose phase velocities equal the load velocity. The wave train with frequency p_1 is in the region ahead of the load front to the point moving with the group velocity $(x/\tau)_1$, while the train with frequency p_2 is behind the load in the region ahead of the point moving with the group velocity $(x/\tau)_2$.

When the load velocity is less than the minimum phase velocity, the poles are complex, but still we have the residue from p_1 ahead of the load and that from p_2 behind the load. These give a solution which decreases exponentially with the distance from the load discontinuity in a manner similar to the response of the beam to a static load.

The simple analytic expression which gives this behavior just discussed can be obtained by using a modification of the saddlepoint analysis due to van der Waerden [3]. The integrand is considered to be a function of the saddlepoint variable u, and is given partial-fractions decomposition which explicitly shows the pole terms and a remainder term.

$$\frac{\alpha(\zeta')\,dp}{p(\zeta')^2[(p\xi')^2-(\zeta')^2]} = \frac{1}{2}\Bigg[([1-4(\xi')^4]^{-\frac{1}{2}}+1)\frac{\alpha(p_1\xi')}{u-u(p_1)} - ([1-4(\xi')^4]^{-\frac{1}{2}}-1)\frac{\alpha(p_2\xi')}{u-u(p_2)}\Bigg] \times du + R\,dp.$$

The pole terms can be integrated exactly, while the remainder term can be shown by the usual saddlepoint estimate to be $0(\lambda^{-\frac{1}{2}})$ uniformly for all positive values of x and τ.

Thus we obtain

$$\frac{1}{2\pi}\operatorname{Im}\int \frac{e^{\lambda(p\tau-\zeta)}\alpha(\zeta')}{p(\zeta')^2[(p\xi')^2-(\zeta')^2]}\,dp = \tfrac{1}{2}\operatorname{Re}[\pm([1-4(\xi')^4]^{-\frac{1}{2}}+1)\,e^{\lambda p_1(\tau-\xi)}\alpha(p_1\xi')I[\pm\lambda^{\frac{1}{2}}u(p_1)] \pm(-[1-4(\xi')^4]^{-\frac{1}{2}}+1)\,e^{\lambda p_2(\tau-\xi)}\alpha(p_2\xi')I[\pm\lambda^{\frac{1}{2}}u(p_2)]] + 0(\lambda^{-\frac{1}{2}}) \tag{8}$$

where

$$I(z) = \pi^{-\frac{1}{2}}\,e^{i\pi/4}\int_{-\infty}^{z} e^{-ix^2}\,dx$$

is a combination of Fresnel integrals, or the complementary error function of a complex argument, and is shown in Fig. 4 for real argument. For the $\pm$ sign in (8), the upper sign is used when the integration contour is γ and the lower for the contour β. Thus, for instance, for points between the load and the point $x/\tau = (x/\tau)_1$ the pole p_1 is above the saddle point

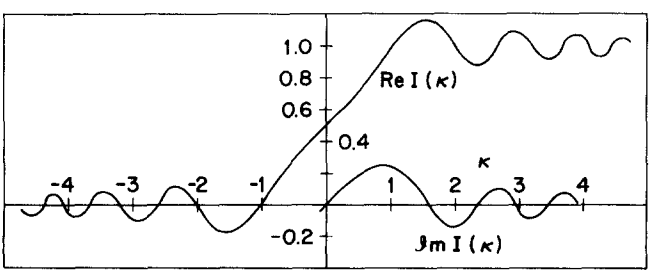

FIG. 4. The function $I(\kappa)$; Note: $\operatorname{Im} I(\kappa) = -\operatorname{Im} I(-\kappa)$.

so $u(p_1)$ is positive, $I[\lambda^{\frac{1}{2}}u(p_1)]$ is approximately unity, and we have the residue from p_1. For p_s in the neighborhood and then above p_1, the I function gives the transition from the head wave train to a dispersive behavior. The results similar to (8) for the moving concentrated load are shown in Fig. 5 for load speeds $(2^{\frac{1}{2}}\xi')^{-1} = 0{\cdot}95$, $1{\cdot}1$ and for the "critical" $1{\cdot}0$, for which (8) increases with the square root of the distance of the load front from the beam end.

Timoshenko beam

To include the effects of transverse shear deformation and rotary inertia, the terms $0(\lambda^{-2})$ of the **A** and **B** in (2) are retained. The complementary solution is

$$\bar{\mathbf{v}} = f(p)\,\mathrm{e}^{-\lambda\zeta(x)}\begin{bmatrix} -(\zeta')^2 \\ \zeta'[(\zeta')^2 - p^2/\lambda^2] \\ \zeta' \\ 1 - \dfrac{\mu}{\lambda^2}[(\zeta')^2 - p^2/\lambda^2] \end{bmatrix} = f(p)\,\mathrm{e}^{-\lambda\zeta}\boldsymbol{\alpha}(\zeta')$$

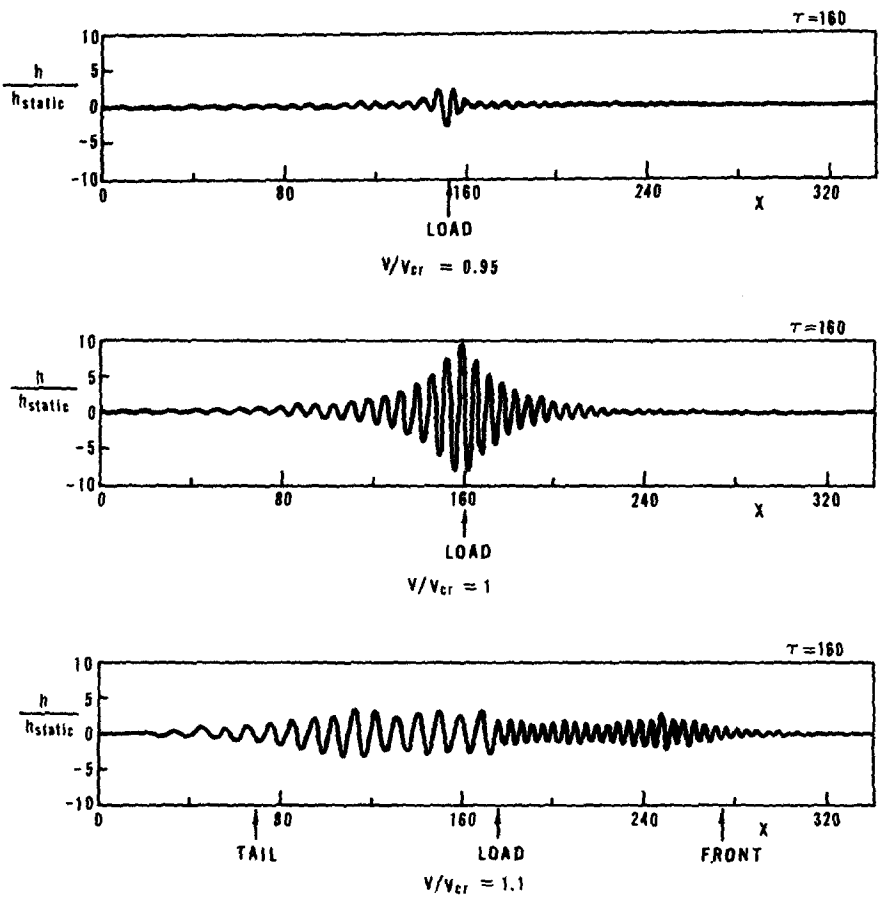

FIG. 5. Deflection of beam with foundation with moving concentrated load.

where f is an arbitrary function and ζ' is a root of the polynomial

$$(\zeta')^2[(\zeta')^2 - p^2/\lambda^2] + (1+p^2)\left(1 - \frac{\mu}{\lambda^2}[(\zeta')^2 - p^2/\lambda^2]\right) = 0.$$

We choose for $\zeta_1'(p)$ the root which has the branch cuts chosen to give the mapping indicated in Figs. 1(a), (b), and which has the behavior

$$\zeta_1' \sim \mu^{\frac{1}{2}} p/\lambda \quad \text{as} \quad p \to \infty, 0 \leq \arg p \leq 2\pi$$
$$\zeta_1'(\bar{p}) = \bar{\zeta}_1'(p), \qquad \zeta_1'(-p) = -\zeta_1'(p).$$

For the root $\zeta_2'(p)$ the branch cuts are chosen to give the mapping shown in Figs. 1(c), (d), which gives the behavior

$$\zeta_2' \sim p/\lambda \quad \text{as} \quad p \to \infty, 0 \leq \arg p \leq 2\pi$$
$$\zeta_2'(\bar{p}) = \bar{\zeta}_2'(p), \qquad \zeta_2'(-p) = -\zeta_2'(p).$$

When p and $\zeta(p)$ are both imaginary, the complementary solution gives a wave train, the phase and group velocities for which are sketched in Fig. 7. For large λ, the curves from the root ζ_1 are the same as for the Euler–Bernoulli beam, shown in Fig. 3, for velocities which are sufficiently smaller than the shear wave velocity $\lambda/\mu^{\frac{1}{2}}$. The root ζ_2' gives a high frequency wave (absent from the E–B beam model) whose (dimensionless) phase and group velocities approach λ, i.e. the bar velocity.

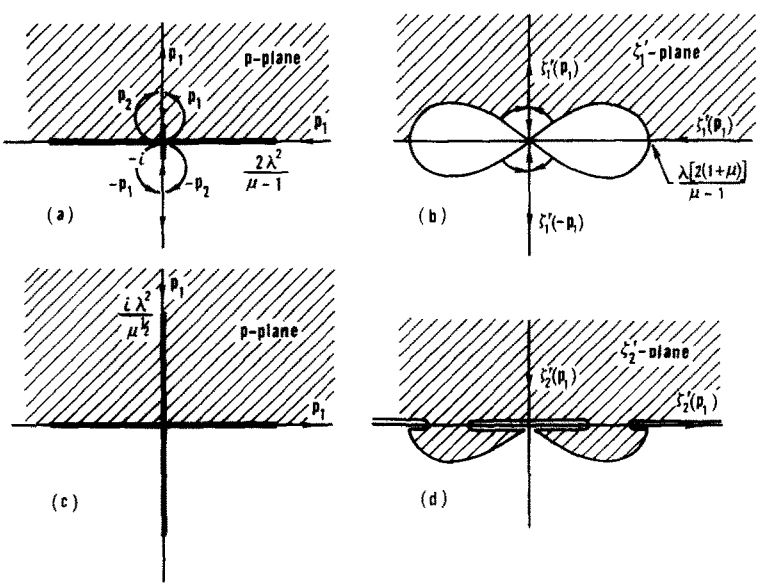

FIG. 6. Mappings for Timoshenko beam.

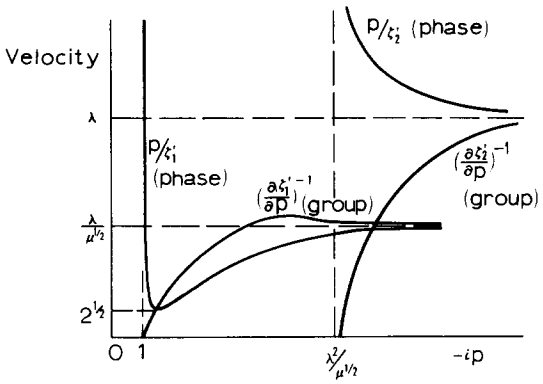

FIG. 7. Wave velocities for Timoshenko beam.

The solution of (3) for the simply-supported semi-infinite beam is in nearly the same form as (6)

$$\bar{v} = \frac{e^{-\lambda p\xi}\alpha(p\xi')}{\lambda p[(p\xi')^2-(\zeta_1')^2][(p\xi')^2-(\zeta_2')^2]} - \frac{e^{-\lambda\zeta_1}\alpha(\zeta_1')}{\lambda p[(p\xi')^2-(\zeta_1')^2][(\zeta_1')^2-(\zeta_2')^2]} - \frac{e^{-\lambda\zeta_2}\alpha(\zeta_2')}{\lambda p[(p\xi')^2-(\zeta_2')^2][(\zeta_2')^2-(\zeta_1')^2]}. \quad (9)$$

The poles of the particular solution (which are exactly cancelled by poles in the complementary solutions) occur at values of p for which $p\xi' = \zeta_1'$ and at $p\xi' = \zeta_2'$. Similar to the E–B beam, the functions $p\xi'+\zeta_1'$ and $p\xi'+\zeta_2'$ do not have any zeros, and the zeros p_1 and p_2 of $p\xi'-\zeta_1'$ have the loci shown in Fig. 6(a). But as the load velocity approaches the shear velocity, p_1 goes to infinity and for larger velocities is on the real p-axis, approaching the branch point $2\lambda^2(\mu-1)^{-1}$. As the load velocity continues to increase, p_1 becomes a zero of $p\xi'-\zeta_2'$ shown in Fig. 6(c), goes to $p = +\infty$ and reappears on the imaginary axis for load speeds in excess of the bar velocity. Unlike the E–B beam, when p_1 and p_2 are zeros of $p\xi'-\zeta_1'$ then $-p_1$ and $-p_2$ are also zeros.

When (9) is inserted in the inversion integral, it is immediately seen that the three terms give zero contribution when the point x under consideration is ahead of the load, ahead of the point moving with the shear velocity, and ahead of the point moving with the bar velocity, respectively. For points behind the load front, we again obtain just the residues from the poles of the particular solution, which can be accounted for by shifting the integration contour of the complementary solution from γ to a contour β to the left of all the poles (but still to the right of the branch cut). Also, since $\zeta_{1,2}(\bar{p}) = \bar{\xi}_{1,2}(p)$ the integral on a contour symmetric about the real p-axis is equal to $2i$ times the imaginary part of the integral over the portion of the path in the upper p-plane. The inversion integral thus reduces to a form similar to (7) but with the sum of two such integrals, one with ζ replaced by ζ_1 and one with ζ replaced by ζ_2, and with the integration contour from a point on the positive real axis to infinity in the upper-half plane.

The results are indicated in Fig. 8. For the load speeds much less than the shear wave velocity, the integral involving ζ_1 is the same as for the E–B beam while that involving ζ_2 is small, giving essentially the E–B results in Figs. 8(b), (c). For higher load speeds, the trailing

wave train remains essentially that indicated by the E–B solution, but significant changes occur in the head wave train. As the load speed approaches the shear velocity, the group velocity also approaches the shear velocity so the head wave train becomes of a more limited length. Then for load speeds in excess of the shear velocity, the pole p_1 is on the real axis, giving an exponentially decreasing function behind the load [Fig. 8(d)]. Finally, for load speeds greater than the bar velocity, the pole p_1 returns to the imaginary axis, but the corresponding group velocity is less than the load velocity, so both the long and short wave length trains are behind the load [Fig. 8(e)].

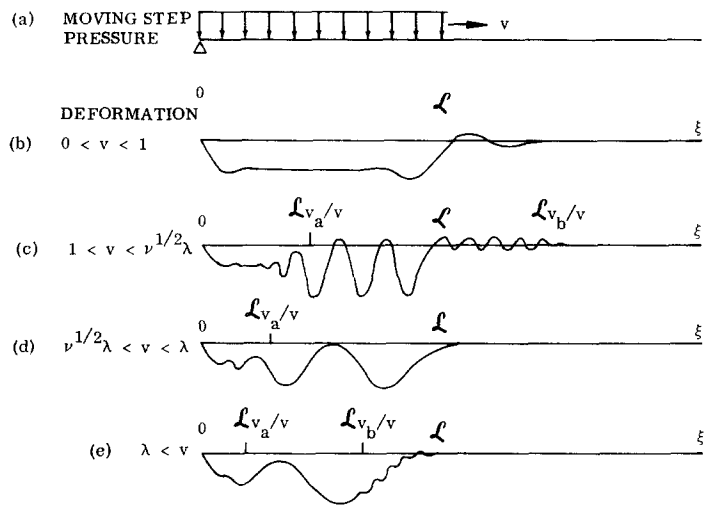

FIG. 8. Deformation of Timoshenko beam for various ranges of load speed.

When the load speed exactly equals the shear or bar velocity care must be used since the pole point is at infinity. However, a reasonably simple approximate solution can be obtained in terms of a Bessel function [6]. The important fact is that the solution is well-behaved, without any resonance buildup, so the sonic speeds are not "critical" even though a "steady-state" solution, i.e. dependent on only the distance from the load discontinuity, is never attained.

Cylindrical shell

The complementary solutions of (3) for the cylindrical shell are of the form

$$\bar{\mathbf{v}} = f(p)\,\mathrm{e}^{-\lambda\zeta(x)} \begin{bmatrix} -(\zeta')^2[\ ] \\ \zeta'[\ ]^2 \\ -\dfrac{\nu p^2}{\lambda}\{\ \} \\ \zeta'[\ ] \\ [\ ]\{\ \} \\ (\nu\zeta'/\lambda)\{\ \} \end{bmatrix} = f(p)\,\mathrm{e}^{-\lambda\zeta}\boldsymbol{\alpha}(\zeta') \tag{10}$$

where, to avoid the introduction of more symbols, we have written

$$[\,] = \left[(\zeta')^2 - \frac{p^2(1-\nu^2)}{\lambda^2}\right]$$

$$\{\,\} = \left\{1 - \frac{\mu}{\lambda^2}\left[(\zeta')^2 - \frac{p^2(1-\nu^2)}{\lambda^2}\right]\right\}.$$

The polynomial for ζ' is now†

$$(\zeta')^2[\,]^2 + \{\,\}\left(-\nu^2\frac{p^2}{\lambda^2} + (1+p^2)[\,]\right) = 0. \tag{11}$$

The behavior of the algebraic function $\zeta'(p)$ defined by this cubic equation can be determined by finding first the relation between phase velocity u and ζ' by replacing p with $u\zeta'$ in (11). The expression reduces to a quadratic, giving the solution

$$-(\zeta')^2 = \frac{\left\{u^2 - \frac{\mu}{\lambda^2}\left(1-\frac{u^2}{\lambda^2}\right) \pm \left[\left(u^2 - \frac{\mu}{\lambda^2}\left(1-\frac{u^2}{\lambda^2}\right)\right)^2 - 4\left(1-\frac{u^2(1-\nu^2)}{\lambda^2}\right)\left(1-\frac{\mu u^2}{\lambda^2}\right)\right]^{\frac{1}{2}}\right\}}{2\left[1-\frac{u^2(1-\nu^2)}{\lambda^2}\right]\left(1-\frac{u^2\mu}{\lambda^2}\right)}.$$

For $u^2 \gg 4$, the two solutions are

$$-(\zeta')^2 \approx \frac{u^2}{\left[1-\frac{u^2(1-\nu^2)}{\lambda^2}\right]\left(1-\frac{\mu u^2}{\lambda^2}\right)}$$

$$-(\zeta')^2 \approx \frac{1-\frac{u^2}{\lambda^2}}{u^2\left[1-\frac{u^2(1-\nu^2)}{\lambda^2}\right]}$$

which easily give the curves of Fig. 9, except near the minimum of p/ζ'_1. When the wave velocities for the Timoshenko beam are plotted as functions of wave number instead of frequency, as in Fig. 8, and the constant phase velocity line of the axial mode is added, curves very similar to those of Fig. 9 are obtained. The essential difference is in the interaction of axial and bending waves in the cylinder. Instead of continuing to infinity as $-i\zeta' \to 0$, the phase velocity of the first mode approaches the bar velocity. Just from Fig. 9, one would expect the cylinder response to the moving load to be generally similar to that for the Timoshenko beam, except for load speeds approaching the bar velocity. In this situation, the group velocity of the trailing wave train also approaches the bar velocity, so all the transient effects will be localized near the load front.

To proceed with the analysis of (11), we note that when $p = 0(1)$, the roots are approximately

$$(\zeta')^2 \approx \pm(-1-p^2)^{\frac{1}{2}}$$

† It should be noted that the more accurate constitutive relations give a modification of the coefficients of the polynomial $0(\lambda^{-2})$, as shown in [11].

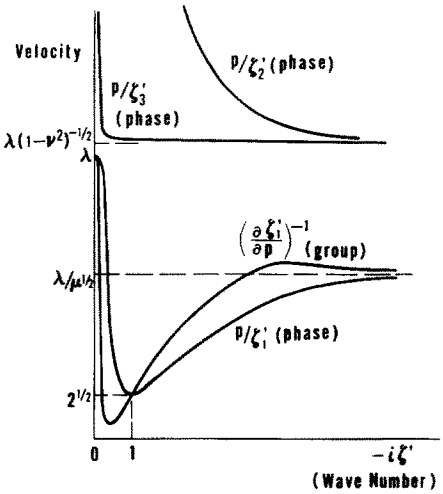

FIG. 9. Wave velocities for cylinder.

and

$$(\zeta')^2 \approx \frac{p^2}{\lambda^2} \frac{p^2(1-\nu^2)+1}{p^2+1}$$

the first of which gives the "bending" and the second the "membrane" behavior. By considering the discriminant of the cubic, repeated roots are found at

$$p^2 \approx \frac{4\lambda^4}{(\mu-1+\nu^2)^2}$$

at

$$p^2 \approx -1$$

and at two conjugate complex points near $p^2 = -1$. Thus the curve of Fig. 10 indicating the behavior of ζ^2 for real values of p^2 is obtained.

The third quadrant of Fig. 10 gives the curves of Fig. 9. In particular, the lower curve gives ζ_1'. This function is single-valued and analytic for real and imaginary values of p, but has different values for $p \to \infty$. So for a function analytic at infinity the branch cuts are chosen as shown in Fig. 11(a). On the outside of the branch cuts the behavior is essentially that of the root ζ_1' for the Timoshenko beam shown in Figs. 6(a), (b). For the cylinder, however, we have the analytic continuation along the imaginary axis inside the branch cut producing a mapping something like that shown in Fig. 11(b).

For the functions ζ_2' the cuts and mapping remain similar to that shown in Figs. 6(c), (d) for the beam. For the function ζ_3' the cuts are shown in Fig. 11(c); the mapping of the p on the ζ_3'-plane is multivalued and cannot be represented by a simple sketch. The important point is that (11) describes three analytic functions of p, all of which are analytic at infinity, have the property $\zeta(\bar{p}) = \bar{\zeta}(p)$, have a positive real part for p real and positive, and have simple approximations in the various regions.

We now may proceed with the solution. Since we have the form of the complementary solution (10) of the transformed equation (3), the particular solution for the engulfing step

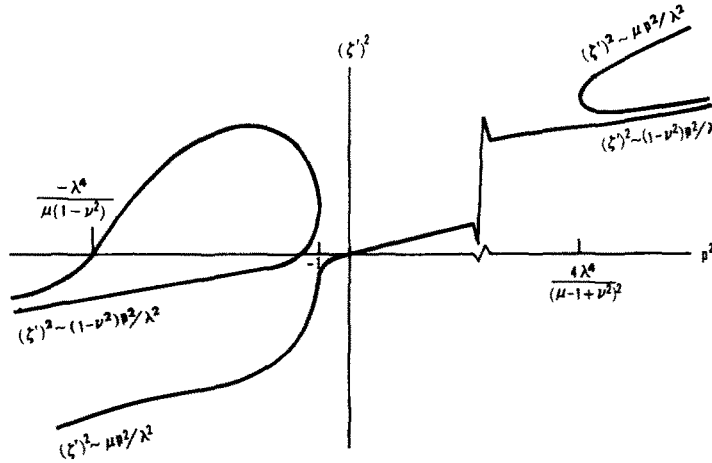

FIG. 10. Behavior of $\zeta^2(p^2)$ for real p^2.

transverse pressure load which satisfies the simple support condition is found to be

$$\begin{aligned}\bar{v} = &\frac{e^{-\lambda p\xi}\alpha(p\xi')}{\lambda p[(p\xi')^2-(\zeta_1')^2][(p\xi')^2-(\zeta_2')^2][(p\xi')^2-(\zeta_3')^2]}\\ &-\frac{e^{-\lambda\zeta_1}\alpha(\zeta_1')}{\lambda p[(p\xi')^2-(\zeta_1')^2][(\zeta_1')^2-(\zeta_2')^2][(\zeta_1')^2-(\zeta_3')^2]}\\ &-\frac{e^{-\lambda\zeta_2}\alpha(\zeta_2')}{\lambda p[(p\xi')^2-(\zeta_2')^2][(\zeta_2')^2-(\zeta_1')^2][(\zeta_2')^2-(\zeta_3')^2]}\\ &-\frac{e^{-\lambda\zeta_3}\alpha(\zeta_3')}{\lambda p[(p\zeta')^2-(\zeta_3')^2][(\zeta_3')^2-(\zeta_1')^2][(\zeta_3')^2-(\zeta_2')^2]}.\end{aligned} \tag{12}$$

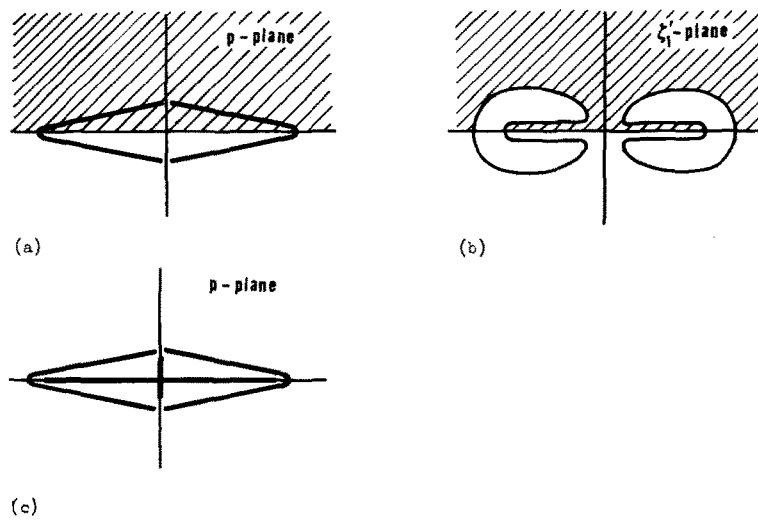

FIG. 11. Mappings for cylinder.

The function (12) when placed in the inversion integral yields integrals similar to those for the Timoshenko beam, giving, as expected, the general behavior similar to that for the Timoshenko beam indicated in Fig. 8. However, when the load speed approaches the bar velocity, the transition of the mode given by ζ_1' from a bending to an axial membrane type of deformation causes a drastic modification of the solution. If we take the load velocity exactly equal to the bar velocity $\xi' = \lambda^{-1}$, it is most convenient to deform the integration contour γ in Fig. 11(a) to the contour β just to the right of the imaginary axis. All the integrations along the branch cuts cancel, while the integrals involving ζ_2 and ζ_3 along the imaginary axis give a small contribution. The contour for the integral of the particular solution may be deformed to $-\infty$ for points behind the load, leaving the residue at $p = 0$. Thus for points just ahead of the load the significant part of the solution comes from the vicinity of the pole.

$$\mathbf{v} \approx -\frac{1}{2\pi i}\int_{\beta} \begin{bmatrix} -(p\lambda^2)^{-1} \\ v^2/\lambda^3 \\ -\lambda/vp^3 \\ \lambda/p^2 \\ 1/p^3 \\ 1/vp^4 \end{bmatrix} e^{(\lambda\tau - x)p + (v^2/2)xp^3}\, dp$$

while for points behind the load front the residue from the particular solution is added.

To evaluate this integral, consider the function

$$G_n(Z, \omega_0) = \int_{-|\varepsilon|-\infty}^{-i|\varepsilon|+\infty} \exp\left\{i(Z\omega) - \frac{\omega^3}{3}\right\} \frac{d\omega}{(\omega-\omega_0)^n}.$$

For $n = 0$, we have the Airy function

$$G_0(Z, \omega_0) = 2\pi Ai(-Z)$$

while for $n = 1$, one can show that

$$G_1(Z, \omega_0) = 2\pi i \int_{-\infty}^{Z} e^{i\omega_0(Z-s)} Ai(-s)\, ds.$$

The formula for general n is

$$G_n(Z, \omega_0) = \frac{1}{(n-1)!} \frac{\partial^{(n-1)}}{\partial \omega_0^{(n-1)}} G_1(Z, \omega_0).$$

In particular

$$G_3(Z, 0) = -i\pi\left[Z^2 \int_{-\infty}^{Z} Ai(-s)\, ds - ZAi'(-Z) + Ai(-Z)\right].$$

With the use of these functions, one finds that only the axial stress, given by the third element of $\mathbf{v}$, is significant

$$v^{(3)}/\lambda = V/E\delta \approx -\frac{1}{2v}\left(\frac{3v^2x}{2}\right)^{\frac{1}{3}} G_3^*(Z)$$

where

$$Z = \left(\frac{2}{3xv^2}\right)^{\frac{1}{3}}(\lambda\tau - x)$$

$$G_3^*(Z) = -\frac{1}{\pi i}G_3(Z,0) - \begin{Bmatrix} 0 & \text{for } Z > 0 \\ Z^2 & \text{for } Z < 0 \end{Bmatrix}.$$

The function $G_3^*(Z)$ is real-valued, dies out exponentially for $Z < 0$, that is, for points ahead of the load front, reaches a maximum of 0·455 at $Z = 0{\cdot}388$, then has damped oscillations for increasing Z. Thus the ratio of maximum dynamic to static stress is

$$\left(1 - \frac{v}{2}\right)\frac{0{\cdot}455}{2v}\left(\frac{3v^2x}{2}\right)^{\frac{1}{3}} = 0{\cdot}17x^{\frac{1}{3}} \quad \text{for } v = 0{\cdot}3.$$

So the stress becomes large for cylinders whose length is in great comparison with the radius. Therefore, the bar velocity is a "critical" load velocity in the same sense as the minimum phase velocity. It seems that the conclusion tentatively offered in [6]—"the only truly critical load speeds are equal to extremums of the phase velocity curve which occur at a finite wave number"—is valid for the cylinder since the bar velocity is a maximum of the phase velocity of the first mode.

INHOMOGENEOUS PROBLEM

For beams and shells with material and/or geometric properties which vary with the spatial coordinate (but not with respect to time), the Laplace transformation in the time variable of the equation (2) may be performed which gives the equation (3). Now, however, since the coefficients and right-hand side of (3) vary with respect to the independent variable, a simple "closed-form" solution is generally not possible. Even the restricted class of variation of the coefficients, for which a solution can be found in terms of some hypergeometric function, is usually not extremely interesting either because the variation is too special or the function is incompletely tabulated and in such a form that does not permit a simple visualization of the results. What seems to be the more fruitful approach is to utilize the methods of asymptotic expansions which have been successfully applied to many problems of shell statics. Of course, similar expansions are used in almost every area of mathematical physics and in particular for the analysis of steady-state solutions of the inhomogeneous wave equation [12]. In the shell statics problem, the large parameter in the equation used for the expansion is the radius-to-thickness ratio (λ^2) while in the wave propagation problems of [12] the expansions are valid for high frequency. For the steady-state vibration of shells, both the radius-to-thickness and frequency parameters must be contended with. Various portions of the problem have been dealt with successfully, as in [13–15].

For the present problem, we need not only the solution of (3), which contains the vibration or steady-state wave propagation solutions, but must use this in the inversion integral to obtain the transient behavior due to the moving load. Such a procedure was successful for the less difficult problem of the propagation of a high-frequency pulse in a bar or slab, described by the inhomogeneous wave equation with one space dimension [9]. The beams and shells presently under consideration are, in contrast, highly dispersive. So, after, using an asymptotic expansion for the solution of the transformed equation (3), it is convenient,

consistent and perhaps necessary, as in the homogeneous case, to use the asymptotic saddlepoint methods to evaluate the inversion integral.

From the preceding discussion of the homogeneous case, it is seen that for load speeds sufficiently less than the shear wave velocity, the essential features of the shell behavior are given by the Euler–Bernoulli beam on an elastic foundation. For simplicity, only a variable foundation will be considered.

Euler–Bernoulli beam

For the beam of constant properties, but with a variable foundation stiffness, with the uniform step load moving at a variable velocity $(\xi')^{-1}$, the transformed equation is (3) with

$$\mathbf{A}+p^2\mathbf{B}=\begin{bmatrix}0&1&0&0\\0&0&0&k^*+p^2\\1&0&0&0\\0&0&-1&0\end{bmatrix}$$

where the ratio of the foundation stiffness to its value at $x = 0$ is $k^* = k^*(x)$. The complementary solutions are sought in the form of an asymptotic series in powers of the large parameter λ

$$\bar{\mathbf{v}}=\mathrm{e}^{-\lambda\zeta(x)}\left[\boldsymbol{\alpha}+\frac{1}{\lambda}\boldsymbol{\alpha}_1+\frac{1}{\lambda^2}\boldsymbol{\alpha}_2+\ \ldots\right] \tag{13}$$

where the $\boldsymbol{\alpha}_i$ are vector functions and $\zeta(x)$ is a scalar, all independent of λ and sufficiently well-behaved. Substitution of (13) into (3) and equating the coefficient of each power of λ to zero give the equations

$$\begin{aligned}(\zeta'\mathbf{I}+\mathbf{A}+p^2\mathbf{B})\,.\,\boldsymbol{\alpha}&=0\\(\zeta'\mathbf{I}+\mathbf{A}+p^2\mathbf{B})\,.\,\boldsymbol{\alpha}_1&=\boldsymbol{\alpha}'\\(\zeta'\mathbf{I}+\mathbf{A}+p^2\mathbf{B})\,.\,\boldsymbol{\alpha}_2&=\boldsymbol{\alpha}_1'\\&\ldots\end{aligned} \tag{14}$$

in which $\mathbf{I}$ is the identity matrix. Therefore $-\zeta'$ must be an eigenvalue of $\mathbf{A}+p^2\mathbf{B}$ and $\boldsymbol{\alpha}$ must be the corresponding eigenvector. For ζ' the polynomial is

$$(\zeta')^4+p^2+k^*=0$$

and we choose the same root as in the homogeneous case which gives the mapping in Fig. 2, except that now the branch points are at $p = \pm i(k^*)^{\frac{1}{2}}$. But now k^* varies with x so we have

$$\zeta=\frac{1+i}{2^{\frac{1}{2}}}\int_0^x (p^2+k^*(x))^{\frac{1}{2}}\,\mathrm{d}x. \tag{15a}$$

The eigenvector is

$$\boldsymbol{\alpha}=f(x,p)\begin{bmatrix}-(\zeta')^2\\(\zeta')^3\\\zeta'\\1\end{bmatrix} \tag{15b}$$

where f is a scalar. Since the matrix in (14) is singular because of the choice for ζ', a solution of the equation for $\boldsymbol{\alpha}_1$ will exist only if the right-hand side is orthogonal to the solution of the homogeneous transpose equation. This condition supplies the equation for f

$$4(\zeta')^3 f' + 6(\zeta')^2 \zeta'' f = 0$$

which has the solution, normalized to be unity at $x = 0$,

$$f = [\zeta'(x)/\zeta'(0)]^{-\frac{1}{2}}. \tag{15c}$$

The solution for $\boldsymbol{\alpha}_1$ is

$$\boldsymbol{\alpha}_1 = \begin{bmatrix} -2 \\ \frac{3}{2}\zeta' \\ \frac{3}{2}(\zeta')^{-1} \\ 0 \end{bmatrix} \zeta'' f + f_1 \boldsymbol{\alpha} \tag{15d}$$

where f_1 is a new scalar function which will be determined from the orthogonality condition on the right-hand side of the equation for $\boldsymbol{\alpha}_2$

$$f_1 = -\frac{1}{2} f \int_0^x \frac{\zeta''}{(\zeta')^2} \, dx. \tag{15e}$$

Similarly the next terms of the expansion may be computed.

If the convergence of the first few terms of (13) is rapid, then the expansion provides an accurate useful approximation to the exact solution of (3). There is one important situation for which the expansion is not valid, and that is when $k^* + p^2$ has one or more zeros on the beam. The terms in (13) are seen to be successively more singular at such a zero. For the homogeneous case, for frequencies $-p^2 < 1$ the root ζ' is complex and dynamic effects are localized, while for frequencies $-p^2 > 1$ the root ζ is real so that the propagation of waves occurs. For k^* variable it is possible to have, for the same frequency of excitation, regions of the beam propagating waves while other regions, in which $-p^2 < k^*$, do not. Such "transition point" behavior is discussed in [13–15]. For the homogeneous moving load problem, however, the interesting transitional behavior occurs at the minimum phase velocity at which the frequency is $-p^2 = 2$, so we encounter in the nonhomogeneous problem at least different transition point problems.

The expansion (13) provides the approximate complementary solutions; a similar expansion with ζ replaced by $p\xi$, which is the argument of the exponent on the right-hand side of (3), will provide an approximate particular solution. However, when the boundary conditions are satisfied and we consider the solution as a function of the transform variable p, the poles of the various terms do not cancel as they do in the homogeneous case. Thus one seeks a better solution to (3).

The first term of (13) $\mathbf{W} = \boldsymbol{\alpha} \, e^{-\lambda \zeta}$ is the exact solution of

$$-\frac{1}{\lambda}\frac{\partial \mathbf{W}}{\partial x} + \left(\mathbf{A} + p^2 \mathbf{B} + \frac{1}{\lambda}\mathbf{C}\right) . \mathbf{W} = 0 \tag{16}$$

where $\mathbf{C}$ is the diagonal matrix

$$\boldsymbol{\alpha}' = \mathbf{C} . \boldsymbol{\alpha}.$$

Thus (3) can be written in the form

$$-\frac{1}{\lambda}\frac{\partial \bar{\mathbf{v}}}{\partial x}+\left(\mathbf{A}+p^2\mathbf{B}+\frac{1}{\lambda}\mathbf{C}\right).\bar{\mathbf{v}}=\frac{1}{\lambda}\mathbf{C}.\mathbf{v}+\frac{e^{-\lambda p\xi}}{\lambda p}\mathbf{b}=\mathbf{R}. \tag{17}$$

Following the method for obtaining error estimates for asymptotic expansions [16] we formally consider the quantity R as known. The solution is

$$\mathbf{v}=\mathbf{W}-\lambda\int^{x}\mathbf{K}(x,X)\mathbf{R}(X)\,dX \tag{18}$$

where the matrix $\mathbf{K}(x, X)$ must satisfy (16) with respect to x and must satisfy the conditions

$$\mathbf{K}(x,x)=\mathbf{I}.$$

If we denote the four complementary solutions by

$$\mathbf{W}_j=\alpha(\zeta_j')\,e^{-\lambda\zeta_j}$$

where

$$\xi_2'=-i\zeta_1', \qquad \zeta_3'=-\zeta_1' \quad \text{and} \quad \zeta_4'=-\zeta_2',$$

then a suitable kernel is formed using the complementary solutions as column vectors

$$\mathbf{K}(x,X)=[\mathbf{W}_1(x)\mathbf{W}_2(x)\mathbf{W}_3(x)\mathbf{W}_4(x)].[\mathbf{W}_1(X)\mathbf{W}_2(X)\mathbf{W}_3(X)\mathbf{W}_4(X)]^{-1}.$$

Since $\mathbf{R}$ actually contains the unknown $\bar{\mathbf{v}}$, (18) is a Volterra integral equation for which the method of successive approximations converges to the solution. So for the first approximation, the nonhomogeneous term is used

$$\bar{\mathbf{v}}\approx-\frac{1}{p}\int^{x}\mathbf{K}(x,X).\mathbf{b}\,e^{-\lambda p\xi(X)}\,dX. \tag{19}$$

Substitution of this into the right-hand side of (18) gives a correction which is generally of the relative size $0(\lambda^{-1})$. So we proceed with the use of the approximation (19), bearing in mind that if we end up with ridiculous results a more careful study of the limitations on (19) should be made.

When (19) is expanded, we have

$$\bar{\mathbf{v}}\approx-\frac{1}{4p}\int^{x}\left[\mathbf{W}_1(x)\frac{e^{\lambda\zeta_1}}{\zeta_1'}-\mathbf{W}_2(x)\frac{e^{\lambda\zeta_2}}{\zeta_2'}+\mathbf{W}_3(x)\frac{e^{\lambda\zeta_3}}{\zeta_3'}-\mathbf{W}_4(x)\frac{e^{\lambda\zeta_4}}{\zeta_4'}\right]\frac{e^{-\lambda p\xi}}{f(\zeta_1')^2}\,dX.$$

As in the homogeneous case, the terms involving ζ_2 and ζ_4 will contribute the complex conjugate of those involving ζ_1 and ζ_3 to the final result. For the integration limits, since ζ_3 becomes negative for $x\to\infty$ for p positive, we choose $X=\infty$ for the lower limit of the integration of the third and fourth terms. Since ζ_1 is the negative of ζ_3 the choice for the limit on the first two terms should be $X=-\infty$. To define ζ_1 for negative arguments we take $\zeta_1(-X)=\zeta_3(X)$ with the result

$$\bar{\mathbf{v}}(x,p)\approx-\frac{1}{4p}\left[\mathbf{W}_1\int_0^{x}\frac{e^{\lambda(\zeta_1-p\xi)}}{f(\zeta_1')^3}\,dX-\mathbf{W}_1\int_{\infty}^{0}\frac{e^{\lambda(\zeta_3-p\xi)}}{f(\zeta_1')^3}\,dX+\mathbf{W}_3\int_{\infty}^{x}\frac{e^{\lambda(\zeta_3-p\xi)}}{f(\zeta')^3}\,dX\right]+\ldots$$

where the dots denote the similar terms with ζ_2 and ζ_4. Note that the simple support conditions are satisfied, since the first and fourth elements of $\mathbf{W}_1(0)-\mathbf{W}_3(0)$ are zero.

When this expression is placed in the inversion integral, it is immediately seen that the portion of the integrals $\xi^{-1}(\tau) < X$ will give a zero contribution since the contour may be deformed to infinity in the direction of positive p. Thus we have, for points behind the load front $x < \xi^{-1}(\tau)$,

$$\begin{aligned} v(x,\tau) = -\frac{\lambda}{4\pi}\operatorname{Im}\int_\gamma \Bigg\{ & \alpha(\zeta_1')\int_0^x \exp\lambda[p\tau - p\xi(X) - \zeta_1(x) + \zeta_1(X)]\frac{dX}{f(X)(\zeta_1'(X))^3} \\ & + \alpha(\zeta_1')\int_{\xi^{-1}(\tau)}^0 \exp\lambda[p\tau - p\xi(X) - \zeta_1(x) - \zeta_1(X)]\frac{dX}{f(X)(\zeta_1'(X))^3} \\ & - \alpha(-\zeta_1')\int_{\xi^{-1}(\tau)}^x \exp\lambda[p\tau - p\xi(X) + \zeta_1(x) - \zeta_1(X)]\frac{dX}{f(X)(\zeta_1'(X))^3}\Bigg\}\frac{dp}{p} \end{aligned} \tag{20a}$$

and, for points ahead of the load $x > \xi^{-1}(\tau)$,

$$v(x,\tau) = -\frac{\lambda}{4\pi}\operatorname{Im}\int_\gamma \left\{\alpha(\zeta_1')\int_0^{\xi^{-1}(\tau)} e^{\lambda[p\tau - p\xi(X) - \zeta_1(x)]}(e^{\lambda\zeta_1(X)} - e^{-\lambda\zeta_1(X)})\frac{dX}{f(X)(\zeta_1'(X))^3}\right\}\frac{dp}{p}. \tag{20b}$$

At this point the problem may seem somewhat out of hand, since a double integration must be performed. However, we may use the standard asymptotic evaluation of the integrals over the space variable X. As discussed in [16], the significant contribution comes from the endpoints of the interval and from any interior saddlepoints. Integration by parts easily yields the endpoint contributions; the integral of these terms over the γ contour in the p-plane gives only the residue at the pole $p = 0$, which reduces to the results, for points behind the load front,

$$v(x,\tau) = \begin{bmatrix} 0 \\ 0 \\ 0 \\ 1/k^* \end{bmatrix} - \operatorname{Re}\left\{\alpha(\zeta')\,e^{-\lambda\zeta_1} + \frac{1}{2}\alpha(-\zeta_1')\frac{e^{-\lambda[\zeta_1(\xi^{-1}(\tau)) - \zeta_1(x)]}}{[fk^*]_{x=\xi^{-1}(\tau)}}\right\}_{p=0} \tag{21a}$$

and, for points ahead of the load,

$$v(x,\tau) = \operatorname{Re}\left\{\frac{1}{2}\alpha(\zeta_1')\frac{e^{-\lambda[\zeta_1(x) - \zeta_1(\xi^{-1}(\tau))]}}{[fk^*]_{x=\xi^{-1}(\tau)}}\right\}_{p=0}. \tag{21b}$$

Thus the end points of the X integrals in (20) give the static solution. In (21a) is seen the displacement, under the uniform load, which varies because of variation in the foundation modulus, and the exponential "edge-effect" correction at the end of the beam and at the load discontinuity. In (21b) is the edge-effect ahead of the load.

The dynamic effects come from the saddlepoint, which is the point at which the derivative, with respect to the variable of integration, of the argument of the exponent vanishes. In the first integral of (20a) the saddlepoint X_s is at the point for which

$$p\xi'(X_s) = \zeta_1'(X_s). \tag{22a}$$

There are no saddlepoints of the other integrals in (20a) since there are no zeros of

$$p\xi'(X_s) + \zeta_1'(X_s).$$

Retaining only the first term of the saddlepoint expansion gives for (20)

$$v(x,t) \approx -\frac{\lambda}{4\pi}\,\mathrm{Im}\int_{\gamma}\left\{\frac{\alpha(\zeta_1'(x))\,e^{\lambda[p\tau-p\xi(X_s)-\zeta_1(x)+\zeta_1(X_s)]}}{\left[f(\zeta')^3\left(\lambda\dfrac{p\xi''-\zeta''}{2\pi}\right)^{\frac{1}{2}}\right]_{x=X_s}}\right\}\frac{dp}{p}.$$

The saddlepoint of this integral is at the value of p for which

$$\tau-\xi(X_s)=\frac{\partial}{\partial p}(\zeta_1(x)-\zeta_1(X_s)) \tag{22b}$$

which gives the result for the dynamic effects

$$v(x,t)=-\frac{1}{2}\mathrm{Re}\frac{\alpha(\zeta_1'(x))\,e^{\lambda[p_s\tau-p_s\xi-\zeta_1(x)+\zeta_1]}}{p_s f(\zeta')^3\left[-\dfrac{\partial^2}{\partial p^2}(\zeta_1(x)-\zeta_1)(p\xi''-\zeta'')+\left(\xi'-\dfrac{\partial\zeta'}{\partial p}\right)^2\right]^{\frac{1}{2}}} \tag{22c}$$

in which the argument X_s has not been explicitly written.

The interpretation of (22) is the following. Consider a point $x = X_s$ on the beam. As indicated in Fig. 12(a) for the homogeneous case, when the load discontinuity passes the point X_s, two waves are generated. Both waves have a (local) phase velocity equal to the load velocity and frequencies given by the two values of p which satisfy (22a). The significant effect of these two waves propagates from the point X_s with the group velocity; the trace in the x, τ plane is given by (22b).

For the inhomogeneous beam, however, the two "rays" emitting from X_s described by (22b) will generally be curved. And, even when k is constant, if the load speed varies the rays from different values of X_s will be at different angles. So several interesting situations can give rise to a curve which is the envelope of the emitted rays [Fig. 12(b)]. On this curve, called a caustic, the denominator of (22c) vanishes. The accurate solution can be obtained in terms of the Airy integral, since generally the third derivative of the argument of the exponent in the integrand is not zero. Thus instead of the singularity indicated by (22c) on the caustic the actual stress magnitude will be $0(\lambda^{\frac{1}{3}})$. At the cusp of two caustics such as indicated in Fig. 12(b), which occurs when the load speed is equal to the minimum phase velocity of waves that can be emitted at a point, the third derivative of the exponent also vanishes and the intensification of stress and displacement is $0(\lambda^{\frac{1}{4}})$.

When the load speed is less than the minimum phase velocity of waves that can be emitted at a point, the roots p of (22a) will be complex and the result (22c) gives only a local effect.

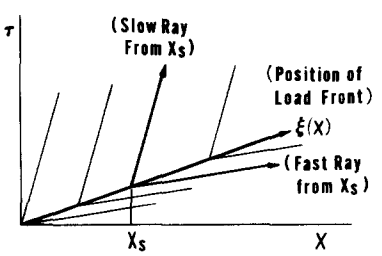

FIG. 12(a). Influence lines for homogeneous case.

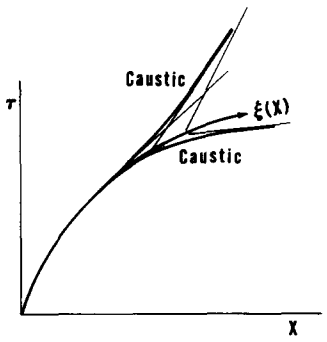

FIG. 12(b). Influence lines for increasing velocity.

If the same argument is used for the cylinder with a variable load speed, the result is similar to Fig. 12. For an increasing load velocity cusps of caustics form when the load passes through the low "critical" velocity and at the "plate" velocity. For a decreasing load velocity, however, caustics form when the load velocity equals the "bar" velocity and the "shear" velocity. Just how significant these caustics are, as far as maximum stress and deflection are concerned, remains to be evaluated.

Thus the results (22) provide a reasonably simple means of computing the general response of the nonhomogeneous beam with a variable load speed, and provide a direct way of identifying regions of stress intensification. Furthermore it is evident that the analysis may be repeated for beams with variable E, A, ρ, or load amplitude with only minor modification, and can be used for the shells of revolution with a variable meridian. The results will be similar to (22) as long as the load speed is sufficiently less than the shear velocity. For the high load speeds, the same general approach should be fruitful, but, as in the case of the cylinder, care must be exercised in the peculiar situations which can arise.

REFERENCES

[1] J. DÖRR, Der unendliche federnd gebettete Balken unter dem Einfluss einer gleichformig bewegten Last. *Ing.-Arch.* **14**, 167–192 (1943).
[2] C. R. STEELE, The finite beam with a moving load. *J. appl. Mech.* **34**; *Trans. Am. Soc. mech. Engrs* **89**, 111–118 (1967).
[3] B. L. VAN DER WAERDEN, On the method of saddlepoints. *Appl. scient. Res.* **2**, 33–45 (1951).
[4] C. R. STEELE, Nonlinear effects in the problem of a beam on a foundation with a moving load. *Int. J. Solids Struct.* **3**, 565–585 (1967).
[5] S. H. CRANDALL, The Timoshenko beam on an elastic foundation, *Proc. of the Third Midwestern Conf. on Solid Mechanics*, Ann Arbor, Mich., pp. 146–159 (1957).
[6] C. R. STEELE, The Timoshenko beam with a moving load. *J. appl. Mech.* **35**; *Trans. Am. Soc. mech. Engrs* **90**, 481–488 (1968).
[7] K. SCHIFFNER and C. R. STEELE, The cylindrical shell with an axisymmetric moving load. *AIAA Jnl* **9**, 37–47 (1971).
[8] G. HERRMANN and E. H. BAKER, Response of cylindrical shells to moving loads. *J. appl. Mech.* **34**; *Trans. Am. Soc. mech. Engrs* **89**, 81–86 (1967).
[9] C. R. STEELE, Asymptotic analysis of stress waves in inhomogeneous solids. *AIAA Jnl* **7**, 896–902 (1969).
[10] H. KRAUS, *Thin Elastic Shells*. Wiley (1967).
[11] P. M. NAGHDI and COOPER, Propagation of elastic waves in cylindrical shells, including the effects of transverse shear and rotary inertia. *J. acoust. Soc. Am.* **28**, 56–63 (1956).
[12] L. M. BREKHOVSKIKH, *Waves in Layered Media*. Academic Press (1960).
[13] E. W. ROSS, JR., Transition solutions for axisymmetric shell vibrations. *J. Math. Phys.* 335–355 (1966).
[14] R. F. HARTUNG and W. A. LODEN, Axisymmetric vibration of conical shells, *Proc. AIAA/ASME Structures Dynamics Specialists Conference*, New Orleans (1969).

[15] P. E. TOVSTIK, Asymptotic integration of the equations of free axisymmetric vibrations of a thin shell of revolution in the case of one turning point. *Inzh. Zh. Mekh. Tverd, Tela* 124–132 (1967).
[16] A. ERDELYI, *Asymptotic Expansion*. Dover (1956).
[17] L. B. FELSEN and N. MARCUVITZ, Modal Analysis and Synthesis of Electromagnetic Fields, Research Report R-776-59, P1B-705, Air Force Cambridge Research Center (1959).
[18] L. I. SLEPYAN, Resonance phenomena in plates and shells with a running load, (in Russian), VI *All-Union Conference on the Theory of Shells and Plates* (1966).
[19] L. I. SLEPYAN, Transitional processes in an elastic layer surrounded by a compressible fluid, (in Russian), *All-Union Symposium*, Tartu, Tallin (1967).
[20] M. W. AISENBERG and L. I. SLEPYAN, Resonance waves in a cylinder submerged in a compressible liquid, (in Russian), *All Union Symposium*, Tartu, Tallin (1967).
[21] M. W. AISENBERG, On the influence of the external medium on the resonance waves in a hollow cylinder, (in Russian). *Arm. SSR Mech.* **22** (1969).
[22] M. W. AISENBERG, On resonance waves in a cylinder, (in Russian). *Eng. J. MTT* No. 1 (1969).

(*Received* 28 *May* 1970; *revised* 11 *November* 1970)

Абстракт—Проверяется переходное состояние балок типа Эйлера–Бернулли и Тимошенки, лежащих на упругом основании, вследствие движущихся нагрузок, используя однако, значительно более простую векторную формулировку, с преобразованием вернее всего Лапласа чем фурье. Показано, что задача цилиндрической оболочки с поглащением осесимметрической волной давления, является, вообще, вполне аналогичной задаче балки Тимошенки. Но даже, в противоположность с балкой Тимошенки, скорость стержня оказывается "критической" скоростью нагрузки, при которой реакция может делаться больше. Это явление возникает вследствиесопряжения между осевым и радиальным движением в цилиндре для типов волн большой длины.

Обсуждается также подход к задачам, в которых изменяются свойства материала и геометрические свойства. Решается преобразованные уравнения методом асимптотических разложений. Затем определяется обратное преобразование Лапласа методом асимптотической седлообразной точки. Каустики, которые являются районами интенсификации напряжений и деформаций, можно получить путем непосредственного численного расчета или с помощью геометрической конструкции.